Electronic Supplementary Material (ESI) for Environmental Science: Nano.

Supporting Information

Core-shell magnetic metal-organic framework molecularly imprinted nanospheres for specific adsorption of tetrabromobisphenol A from water

Minna Li [1 a], Ping Sun [1 a], Qiong Wu [a], Desheng Liu [a], Lincheng Zhou [a,b*]

a. State Key Laboratory of Applied Organic Chemistry, College of Chemistry and Chemical Engineering, Institute of Biochemical Engineering & Environmental Technology, Lanzhou University, Lanzhou 730000, P. R. China.

b. Zhongwei High-tech Institute of Lanzhou University, 755000, P. R. China.

1. These authors contributed equally to this work and should be considered as co-first authors.

Minna Li E-mail: limn16@lzu.edu.cn Fax: 86-0931-8912113 Tel. 86-0931-8912528

Address: College of Chemistry and Chemical Engineering, Lanzhou University, Lanzhou 730000, P.R.China

Ping Sun E-mail: sunp_14@lzu.edu.cn Fax: 86-0931-8912113 Tel. 86-0931-8912528

Address: College of Chemistry and Chemical Engineering, Lanzhou University, Lanzhou 730000, P.R.China

Qiong Wu E-mail: qwu14@lzu.edu.cn Fax: 86-0931-8912113 Tel. 86-0931-8912528

Address: College of Chemistry and Chemical Engineering, Lanzhou University, Lanzhou 730000, P.R.China

Desheng Liu E-mail: liudsh17@lzu.edu.cn Fax: 86-0931-8912113 Tel. 86-0931-8912528

Address: College of Chemistry and Chemical Engineering, Lanzhou University, Lanzhou 730000, P.R.China

Lincheng Zhou E-mail: zhoulc@lzu.edu.cn Fax: 86-0931-8912113 Tel. 86-0931-8912528

Address: College of Chemistry and Chemical Engineering, Lanzhou University, Lanzhou 730000, P.R.China

*Corresponding author. Tel: 86-0931-8912528. E-mail: zhoulc@lzu.edu.cn

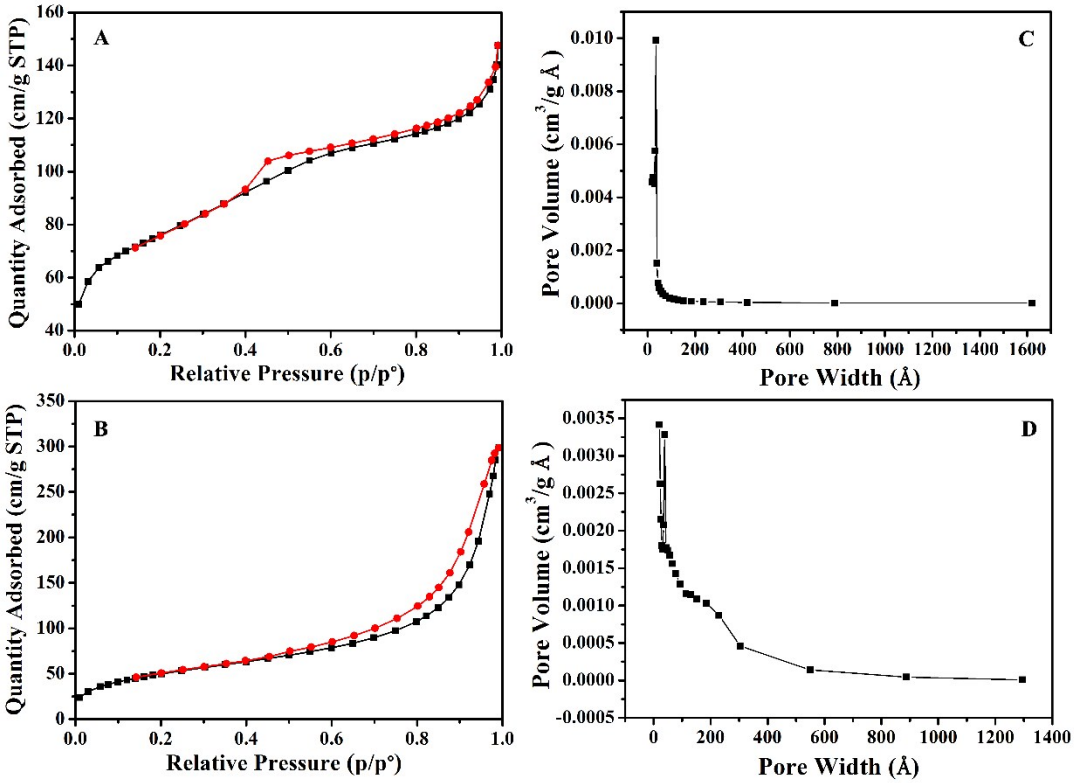

Fig. S1 Nitrogen adsorption-desorption isotherms of Fe_3O_4@ZIF-8 (A) and Fe_3O_4@ZIF-8@MIP (B), the pore size distribution curves of Fe_3O_4@ZIF-8 (C) and Fe_3O_4@ZIF-8@MIP (D).

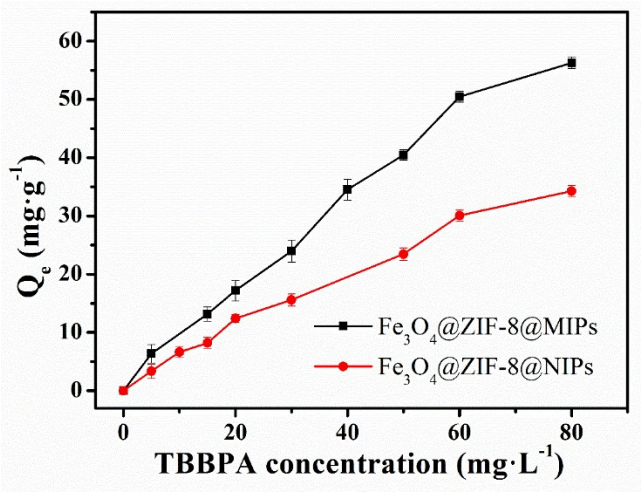

Fig. S2 TBBPA adsorption isotherms of Fe_3O_4@ZIF-8@MIP and Fe_3O_4@ZIF-8@NIP at 303 K.

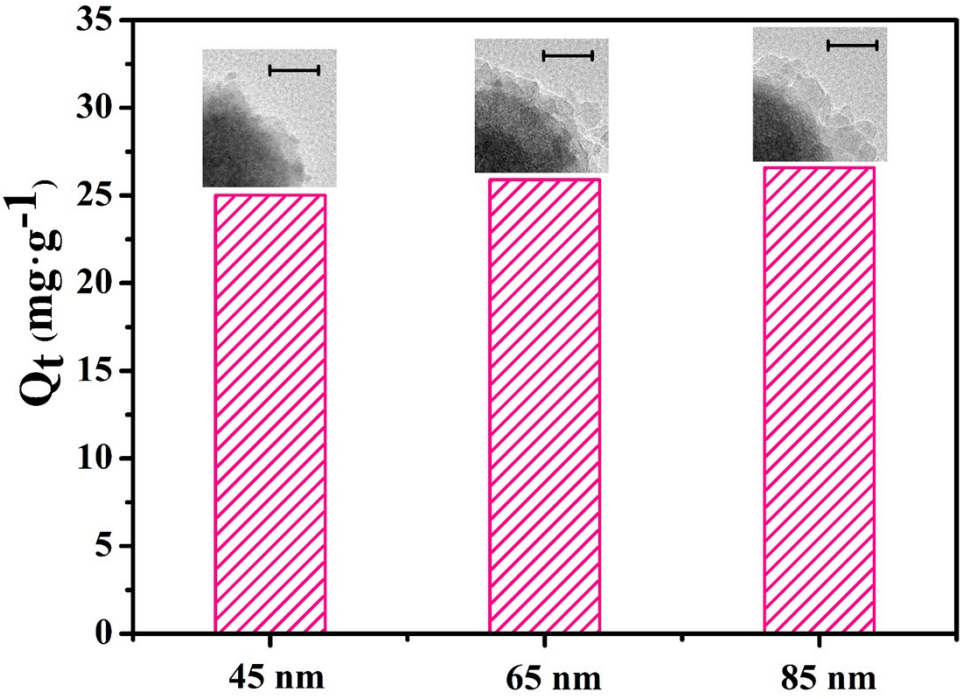

Fig. S3 Adsorption capacity of Fe_3O_4@ZIF-8@MIPs prepared with different thickness of ZIF-8 layer at 303 K (the scale bar in figure is 100 nm).

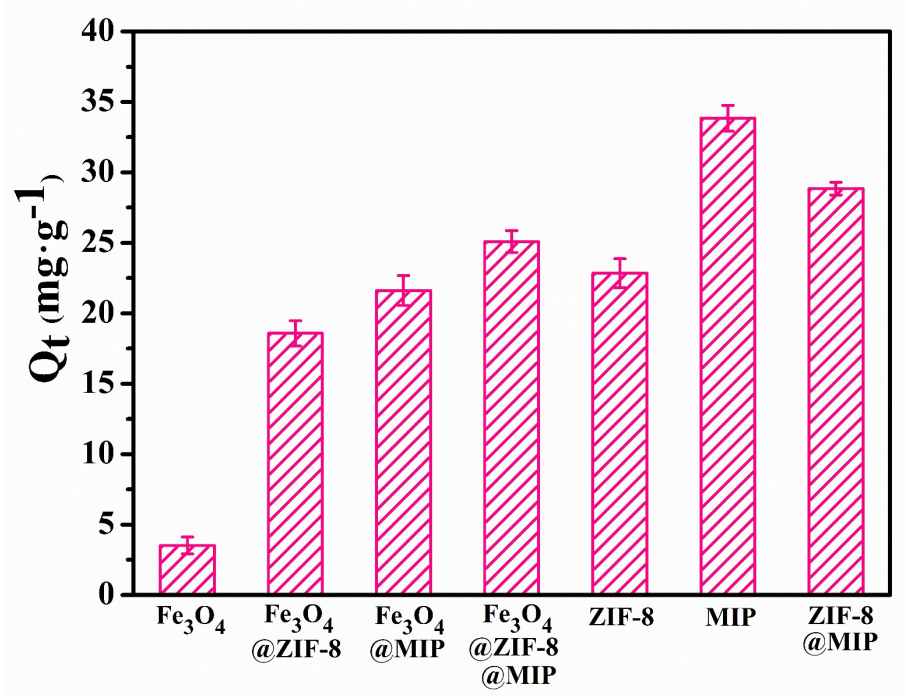

Fig. S4 Adsorption capacity of different adsorbents at 303 K.

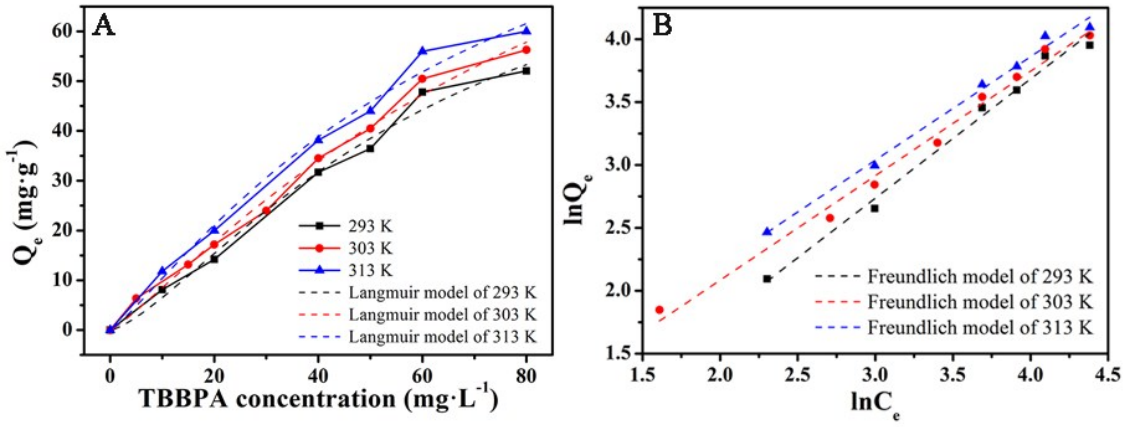

Fig. S5 Adsorption isotherms of Fe_3O_4@ZIF-8@MIP and Fe_3O_4@ZIF-8@NIP at 293, 303 and 313 K, curves fitted by Langmuir model (A) and by Freundlich model (B).

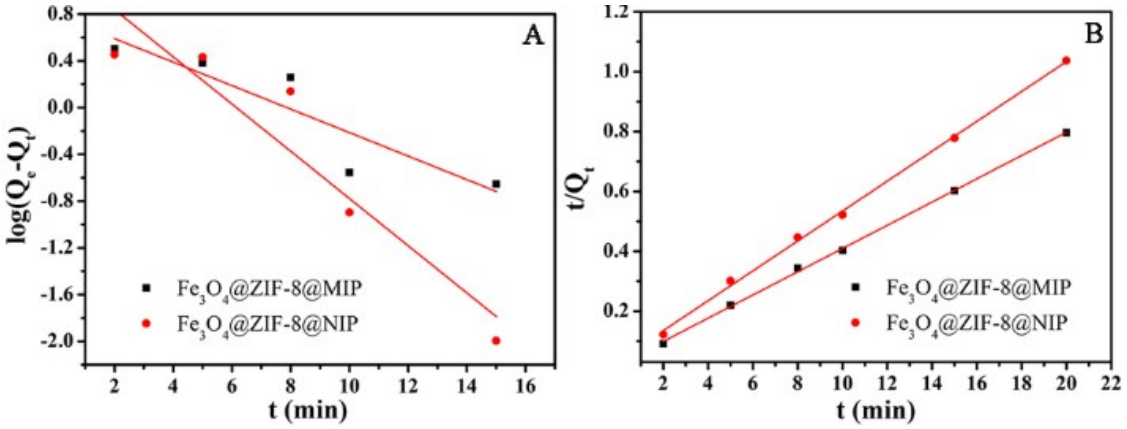

Fig. S6 Pseudo-first-order linear fitting curves (A) and Pseudo-second-order linear fitting curves (B) of Fe_3O_4@ZIF-8@MIP.

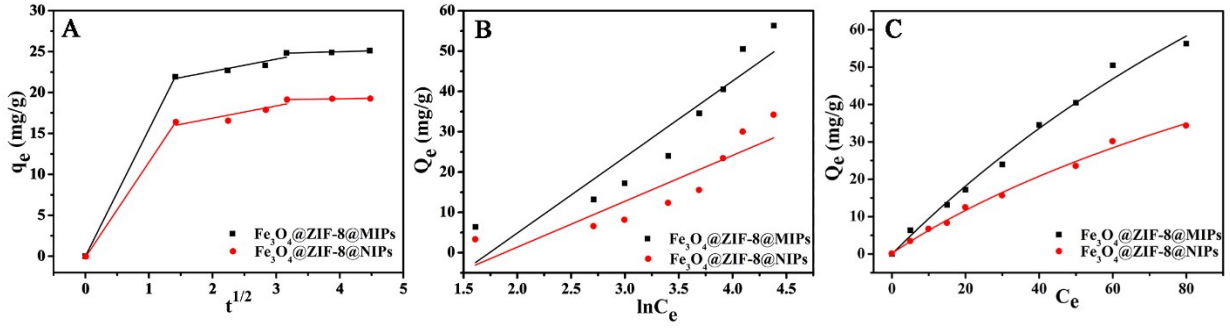

Fig. S7 Various analytical models of Fe_3O_4@ZIF-8@MIPs, Weber and Morris (A), Temkin (B), Redlich-Peterson (C).

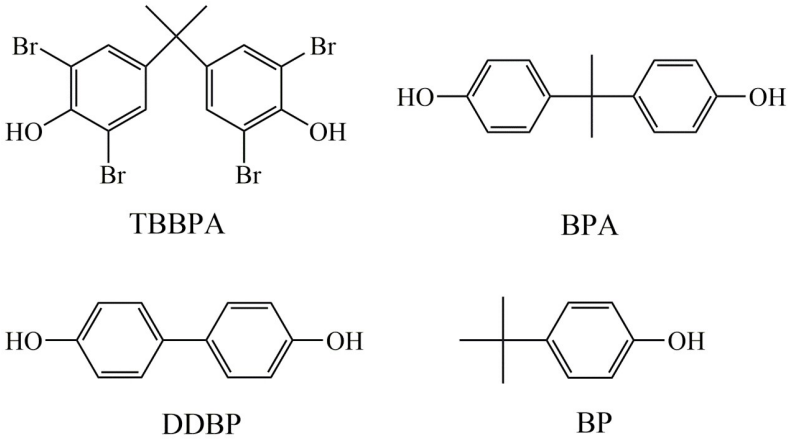

Fig. S8 Structures of TBBPA, BPA, DDBP and BP.

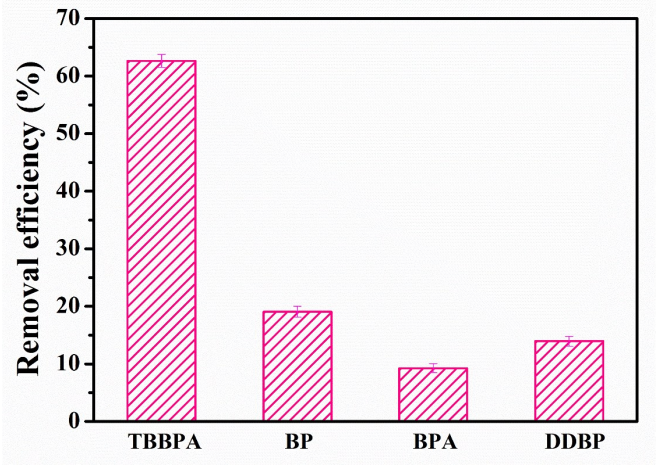

Fig. S9 Competitive adsorption property of Fe_3O_4@ZIF-8@MIP.

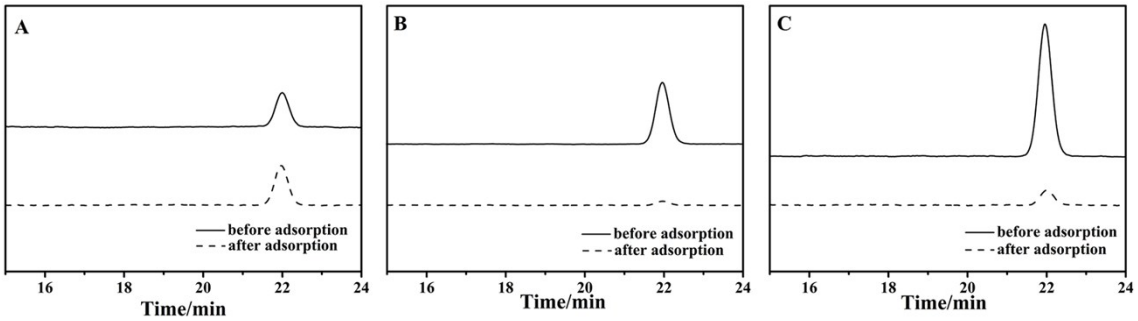

Fig. S10 Chromatography about determination of TBBPA in actual water sample (A: 5 μg/mL, B: 10μg/mL, C: 20 μg/mL).

Table S1 Preparation of MIP and NIP with different methods.

Preparation method	Solvent	Functional monomer:crosslinker	TBBPA adsorption capacity (mg g^{-1})	
			Fe_3O_4@ZIF-8@MIP	Fe_3O_4@ZIF-8@NIP
Radical polymerization	toluene	MAA:TEOS (1:1)	2.094	1.825
	acetonitrile	4-VP:TEOS (1:2.5)	4.396	2.400
	ethanol	DTAP:TEOS (1:10)	4.576	2.903
Sol-gel process	ethanol	APTES:TEOS (1:2)	15.519	9.113

In this work, MAA, 4-VP, di-tert-amyl-peroxide (DTAP) and APTES are chosen as different functional monomers to explore influence of polymerization methods on adsorption capacity. Among these monomers, the formation mechanism of imprinted polymer prepared by APTES and TEOS belongs to sol-gel process, while others belong to radical polymerization. As shown in Table S1, it is obviously noticed that the binding efficiency of MIP synthesized by APTES is superior to other monomers, which can be attributed to strong hydrogen bond interaction between TBBPA and APTES. According to the experiment, APTES is selected as proper functional monomer, and the optimum ratio of APTES and TEOS is 1:2.[1]

Table S2 Isothermal adsorption model parameters of Fe_3O_4@ZIF-8@MIP and Fe_3O_4@ZIF-8@NIP for TBBPA at different temperatures.

Samples	Langmuir				Freundlich		
	T(K)	Q_m (mg g^{-1})	K_L (L mg^{-1})	R^2	K_F ((mg g^{-1}) (L $mg^{-1})^{1/n}$)	1/n	R^2
MIP	293	108.6	0.0031	0.976	0.8986	0.94	0.994
	303	117.6	0.0109	0.985	1.5263	0.83	0.990
	313	120.2	0.0134	0.976	1.7646	0.82	0.990
NIP	293	76.3	0.0121	0.984	0.8179	0.89	0.992
	303	81.0	0.0078	0.980	0.9030	0.84	0.993

	313	85.6	0.0069	0.985	1.0576	0.79	0.988

Table S3 Dynamic model parameters of Fe_3O_4@ZIF-8@MIP and Fe_3O_4@ZIF-8@NIP for TBBPA at 303K.

Samples	Pseudo-first-order				Pseudo-second-order		
	$Q_{e,exp}$ (mg g^{-1})	$Q_{e,cal}$ (mg g^{-1})	k_1 (min^{-1})	R^2	$Q_{e,cal}$ (mg g^{-1})	k_2 (g mg^{-1} min^{-1})	R^2
MIP	25.11	17.46	0.2315	0.767	25.7732	0.0704	0.999
NIP	19.29	6.19	0.4650	0.850	20.0280	0.0710	0.998

Table S4 Various analytical models of Fe_3O_4@ZIF-8@MIPs and Fe_3O_4@ ZIF-8@NIPs.

Samples	Parameters	MIPs	NIPs
Weber and Morris $q_e = K_{WM}\sqrt{t} + C$	K_{WM1}	15.5043	11.6234
	C_1	2.5122×10^{-15}	0
	R2 1	--	--
	K_{WM2}	1.4921	1.4964
	C_2	19.5949	13.9166
	R2 2	0.7902	0.7103
	K_{WM3}	0.2085	0.0989
	C_3	24.1481	18.8631
	R2 3	0.7243	0.6928
Temkin $Q_e = B_t \ln K_t + B_t \ln C_e$	K_t	5.7106	1.0002
	B_t	18.8570	11.3838
	R^2	0.8549	0.7732
Redlich-Peterson $Q_e = \frac{AC_e}{1 + BC_e^{\beta}}$	A	0.6692	0.6692
	B	0.0045	0.0122
	β	1	0.8640
	R^2	0.9883	0.9920

Other analytical models are also investigated in this work. For example, Weber and Morris equation is usually employed to describe mechanism of adsorption as given by:

$$q_e = K_{WM}\sqrt{t} + C \quad (1)$$

In the equation, K_{WM} and C mean the diffusion rate constant (mg/g $min^{1/2}$) and the intercept, respectively. As shown in Fig. S6 (A), it is viewed that the adsorption process can be divided into three parts, and the intraparticle diffusion is not the step that only controlled by rate.[2]

Temkin model presumes that binding energy has a uniform distribution so that can up to the maximum binding energy during the adsorption[3] and is typically used as following:

$$Q_e = B_t \ln K_t + B_t \ln C_e$$

(2)

Where K_t (L mg^{-1}) represents the equilibrium binding constant, corresponding to the maximum binding energy.

Redlich-Peterson model is a three-parameter equation to evaluate the adsorption, describing the adsorption isotherm. It combines the characteristic of the Langmuir and Freundlich isotherms[4, 5], a general equation can be obtained:

$$Q_e = \frac{AC_e}{1 + BC_e^{\beta}}$$

(10)

Where A, B and β are the Redlich–Peterson model isotherm constant (L/g), the model constant (L/mg) and the exponent, respectively. It needs to note that the β lies between 0 and 1. There are two limiting behaviors: Langmuir form for $\beta = 1$ and Henry's law form for $\beta = 0$.[4]

Reference

1. Y. Yin, Y. Chen, X. Wang, Y. Liu, H. Liu and M. Xie, Dummy molecularly imprinted polymers on silica particles for selective solid-phase extraction of tetrabromobisphenol A from water samples, *Journal of chromatography. A*, 2012, 1220, 7-13.
2. S. Hosseini, M. A. Khan, M. R. Malekbala, W. Cheah and T. S. Y. Choong, Carbon coated monolith, a mesoporous material for the removal of methyl orange from aqueous phase: Adsorption and desorption studies, *Chemical Engineering Journal*, 2011, 171, 1124-1131.
3. Y. Kim, C. Kim, I. Choi, S. Rengaraj and J. Yi, Arsenic Removal Using Mesoporous Alumina Prepared via a Templating Method, *Environmental Science & Technology*, 2004, 38, 924-931.
4. E. D. v. Hullebusch, M. H. Zandvoort and P. N. Lens, Nickel and cobalt sorption on anaerobic granular sludges: kinetic and equilibrium studies, *Journal of Chemical Technology &*

Biotechnology, 2004, 79, 1219-1227.

5. F.-C. Wu, B.-L. Liu, K.-T. Wu and R.-L. Tseng, A new linear form analysis of Redlich–Peterson isotherm equation for the adsorptions of dyes, *Chemical Engineering Journal*, 2010, 162, 21-27.